Copy
RM E54E20

NACA

RESEARCH MEMORANDUM

EFFECT OF WEDGE-TYPE BOUNDARY-LAYER DIVERTERS ON PERFORMANCE OF HALF-CONICAL SIDE INLETS AT MACH NUMBER 2.96

By Harry W. Johnson and Thomas G. Piercy

Lewis Flight Propulsion Laboratory
Cleveland, Ohio

NATIONAL ADVISORY COMMITTEE
FOR AERONAUTICS

WASHINGTON
August 2, 1954

NATIONAL ADVISORY COMMITTEE FOR AERONAUTICS

RESEARCH MEMORANDUM

EFFECT OF WEDGE-TYPE BOUNDARY-LAYER DIVERTERS ON PERFORMANCE OF HALF-CONICAL SIDE INLETS AT MACH NUMBER 2.96

By Harry W. Johnson and Thomas G. Piercy

SUMMARY

An experimental investigation was performed at Mach number 2.96 to study the effects of wedge-type boundary-layer removal on the performance of side inlets employing half of a double-conical external-compression surface. Boundary-layer-removal parameters investigated included the wedge height, the wedge included angle, the wedge tip position, and the splitter-plate geometry. Two lengths of constant-area diffuser throat section were considered.

In general, diffuser performance was improved by minimizing the influence of the boundary-layer-removal wedges on the inlet flow. When the boundary-layer wedges were located in their most forward location, increasing inlet pressure recovery was obtained by decreasing the included angle of the boundary-layer-removal wedges. Pressure recovery also increased when the wedges were moved to a rearward position; at this position, however, wedge angle had little effect on inlet pressure recovery.

When the wedges were at the forward position, the configurations having swept-leading-edge splitter plates generally attained higher inlet pressure recovery than those with splitter plates having leading edges normal to the flow direction. However, when the wedges were at a rearward location, splitter-plate configuration had little effect on inlet pressure recovery.

INTRODUCTION

Several systems of boundary-layer removal were investigated at Mach numbers of 1.88 and 2.93 for single-shock external-compression side inlets (ref. 1). Inlet performance for scoop-type boundary-layer removal, wherein the boundary layer ahead of the inlets was taken into a duct and discharged at a downstream station, was compared with wedge-type removal, for which the boundary layer was simply

diverted around the inlet by means of a 62° included-angle wedge. It was found that for wedge heights somewhat larger than the boundary-layer thickness, the wedge diverter yielded inlet peak total-pressure recoveries comparable with those obtained with scoop-type removal. However, for removal heights equal to the boundary-layer thickness, inlet pressure recovery obtained by using the wedge diverter was inferior to that obtained with scoop removal.

From the results of reference 2 it was surmised that the performance of diverter-type side inlets could be improved by minimizing the influence of the wedge on the inlet. This could be accomplished by (1) the use of small-included-angle wedges, (2) moving the wedge rearward so that the apex of the wedge is downstream of the apex of the external-compression surfaces, or (3) both. These parameters have been investigated for two-dimensional ramp-type inlets at Mach numbers of 1.5 to 2.0, and the results are reported in reference 3.

The purpose of this report is to present the results of an experimental investigation to explore the parameters affecting wedge-type boundary-layer removal for half-conical double-shock side inlets at Mach number 2.96. Parameters investigated include (1) wedge-to-boundary-layer thickness ratio, (2) wedge included angle, (3) wedge tip location relative to spike tip position, and (4) splitter-plate geometry. Also investigated was the effect of two lengths of constant-area throat section in the inlet subsonic diffuser. These tests were conducted in the 18- by 18-inch Mach number 3.05 tunnel of the NACA Lewis laboratory.

SYMBOLS

A	area
C_{D_p}	pressure drag coefficient
d	wedge base dimension, 4.88 in.
h	boundary-layer-removal height
h/δ	dimensionless boundary-layer-removal parameter
l	distance from spike tip to wedge tip, 2.34 or 0 in.
l/d	wedge position parameter, dimensionless
m	mass flow

P	total pressure
R	inlet radius, 1.5 in.
V/V_0	ratio of velocity in boundary layer to free-stream velocity
x	axial distance, measured from station 0 (fig. 1)
y	normal distance above flat plate
α_w	included angle of boundary-layer-removal wedge
δ	boundary-layer thickness, distance from flat plate where velocity is equal to 0.99 free-stream velocity
δ^*/θ	boundary-layer form factor, defined by quotient of displacement and momentum thickness

Subscripts:

max	maximum
0	free stream
1	conditions 1/2 in. upstream of spike tip
2	conditions at exit of diffuser
t	throat

APPARATUS AND PROCEDURE

The model for the present test (fig. 1) consisted of half of an axially symmetric inlet mounted on a flat plate. The configuration was similar to that reported in reference 1 except that the model was lengthened upstream of station 5.25 to permit installation of wedge diverters of 30° included angle.

The external-compression surface was a two-shock cone with compression angles of 19.8° and 34.4°, respectively, measured from the free-stream direction. This design allowed a 5° included lip angle and a 2.4° margin in external-flow deflection without lip shock detachment at Mach number 2.96. The theoretical-pressure-recovery ratio of the inlet was 75.1 percent, or only 2 percent below the theoretical optimum design, which was found to be impractical since it allowed only a 1° included lip angle if shock detachment at the lip was to be avoided. The inlet was designed to capture a full stream tube of air with complete boundary-layer removal.

Lengthening the model for inclusion of wedges of 30° half angle also allowed variations in subsonic-diffuser-area distributions. As shown in figure 1, two subsonic-area distributions were investigated; model A incorporated a constant-area section of about 2 inlet radii, while model B had a constant-area section of about two-thirds of the inlet radius. Both models were identical at stations forward of model station 0. Table 1 presents pertinent model dimensions, and figure 2 presents the resulting subsonic-diffuser-area distributions. It may be noted that for both models the area distribution was partially determined according to the criterion of static-pressure gradient proportional to the static pressure (ref. 4).

As indicated in figure 3, 30°, 40°, and 50° included-angle wedges were studied. Provision was made for varying the height of each wedge to obtain varying amounts of boundary-layer removal and for changing the longitudinal locations of the 40° and 50° wedges with respect to the inlet. When the wedges were tested in the most forward position, the wedge and the cone tips coincided at station -3.80. When the 40° and 50° wedges were moved to their downstream location, the wedge tips were positioned at station -1.46.

Two of the splitter-plate configurations tested are indicated in figure 1. The straight-leading-edge plate was normal to the flow direction and was located at the tip of the cone compression surface. The leading edge of the second splitter plate was swept from the cone tip to the lip of the inlet. One additional splitter-plate configuration was investigated briefly; for these tests the splitter-plate leading edge was again normal to the flow direction but was located at the inlet lip. The leading edge of each splitter plate was beveled on the lower side at approximately 9.5° in the streamwise plane.

Inlet total-pressure recovery was obtained with a 41-tube total-pressure rake at the end of the subsonic diffuser. Inlet mass flow was determined by using the average total-pressure recovery and by assuming a choked exit, the area of which was controlled by a remotely operated plug.

Boundary layer was generated on a flat plate that extended 14.5 inches upstream of the spike tip. Carborundum dust was added near the plate leading edge to insure early transition to turbulent flow. The boundary layer 1/2 inch upstream of the spike tip was surveyed with remotely controlled total-pressure probes. The resulting boundary-layer profile and several boundary-layer parameters are presented in figure 4(a). The effect of the boundary layer on the pressure and mass flow in the projected inlet stream tube is presented in figure 4(b). Figure 4(b) thus allows the data presented herein to be referenced to the mass flow and area-weighted total pressure immediately

ahead of the inlet. The test Mach number was reduced to 2.96 by an inclination of the flat plate in the test section of the tunnel.

DISCUSSION OF RESULTS

Inlet Mass-Flow Ratio

Although the inlet was designed to capture a full stream tube of air, less than theoretical mass flow was captured. This discrepancy arose from several factors. In preliminary tests, boundary layer was found to bridge the second compression surface with the result that the second shock was not properly located. When roughness was added near the tip of the first compression surface to eliminate this effect, the first conical shock was displaced slightly. In addition, some inaccuracy was noted in the angle of the second compression surface as compared with the original design and there was the possibility of slight axial misalinement of the compression surfaces due to tolerances of the model. As a result of these factors, a minimum spillage of approximately 5 percent resulted.

Model A, Long Throat

Inlet total-pressure recovery and mass flow are presented in figure 5 for several boundary-layer-removal configurations for the model with the long throat, model A. The straight splitter plate was investigated, and the boundary-layer-removal wedges were located in the forward position (i.e., $l/d = 0$). The usual increase in pressure recovery and mass flow with increase in the boundary-layer-removal parameter h/δ was obtained. In addition, pressure recovery and inlet mass flow increased considerably with decreasing wedge angle α_w. Gains in subcritical stability were also noted for the smaller wedge angles.

The effect of moving the 40° and 50° wedges to their downstream position is indicated in figure 6. By comparing these results with those of figure 5, it is seen that considerable gains in inlet pressure recovery and mass flow were obtained by rearward wedge movement. The gains in inlet peak total-pressure recovery are shown more graphically in figure 7. A pressure-recovery ratio increase of approximately 0.10 was obtained by moving the 50° wedge to its downstream location. Inlet-mass-flow ratio at peak pressure recovery also increased with rearward wedge movement. While significant changes in pressure recovery and mass flow were noted as the wedge angle was changed at l/d of zero, only minor differences appeared when these wedges were moved downstream ($l/d = 0.48$).

[redacted]

Similar data for the swept splitter plate at l/d of zero and 0.48 are presented in figures 8 and 9, respectively. In general, the inlet performance increased with increased boundary-layer removal, decreasing wedge angle, and rearward movement of the wedges, as was observed with straight-splitter-plate configurations. A comparison of these results with those of the straight splitter plate indicate that, for l/d of zero (fig. 5), increases in peak pressure recovery and critical inlet mass flow were obtained by use of the swept splitter plate. At l/d of 0.48 (fig. 6), the peak pressure recoveries and critical mass flows were generally comparable, but the maximum pressure recovery occurred at smaller values of h/δ (0.793) with the swept splitter plate. For this case, a 10-percent margin of subcritical stability was obtained. For both wedge locations, the inlet mass-flow ratio at the maximum-pressure-recovery condition was larger for the swept-splitter-plate configurations. Peak total-pressure recovery for swept-splitter-plate configurations is summarized in figure 10.

In reference 5 similar improvements are noted in side-inlet pressure recovery by sweeping the leading edge of the splitter plate at Mach number 2.75. These data were obtained with a single-shock half-conical inlet with some internal contraction.

A study of the shock structure ahead of the inlet for a straight-splitter-plate configuration is presented in figure 11. A shadowgraph of the flow field in figure 11(a) indicates boundary-layer disturbances ahead of the inlet which interfered with the usual shock pattern. Figure 11(b) presents a photograph of the shock pattern on the main boundary-layer plate obtained after a mixture of machinists' layout blue solution and alcohol was allowed to enter through a plate static tap. (A more complete description of this method of flow visualization may be found in ref. 2). The shock disturbance ahead of the splitter plate is seen to exist across the width of the splitter plate. It was not determined whether this shock wave was separate from the bow wave from the wedge or whether the two had coalesced into a single shock. With this disturbance ahead of the splitter plate, boundary layer presumably flowed over the splitter plate, thus causing the inlet to effectively operate at a lower value of h/δ. Decreasing the shock disturbance ahead of the inlet by decreasing the included wedge angle and by moving the wedges rearward therefore offers an explanation for the performance improvements noted.

A similar study of the shock patterns is presented in figure 12 for swept-splitter-plate configurations. Here, however, comparison is made of the flow fields ahead of the inlet for the two wedge positions investigated. A comparison of shadowgraphs for the two wedge positions shows very little difference. The photographs of the shock traces on the main plate, however, indicate the improvement obtained with the rearward wedge configurations. At l/d of zero, the wedge

shock is seen to disturb the boundary layer well ahead of the inlet lip; however, in figure 12(b) for l/d of 0.48, it is noted that the wedge shock has been moved rearward beneath the splitter plate along with the wedge. Thus the inlet with rearward wedge position was effectively separated from the external boundary layer.

The marked superiority of the swept-splitter-plate configuration over the straight-splitter-plate configuration observed at l/d of zero is not as easily explained. Study of the shock patterns for the straight and swept splitter plates in figures 11 and 12(a), respectively, indicated that for the straight splitter plate the boundary layer would tend to flow up over the width of the splitter plate towards the inlet; for the swept splitter plate, however, most of the disturbed boundary layer is diverted around the inlet by the laterally diverging nature of the flow behind the detatched shock.

One additional splitter-plate variation was investigated following preliminary study by North American Aviation, Inc. For this configuration, the splitter plate was eliminated ahead of the inlet lip. The spike tip was then effectively cantilevered from the inlet since the 40° wedge was installed at its rearward position. The resulting performance (fig. 13) indicated fair subcritical stability and a maximum pressure recovery nearly comparable with that obtained for the swept-splitter-plate configuration. However, inlet mass flow at the maximum-pressure-recovery condition was reduced slightly from that obtained by using the swept-splitter-plate configuration; also a larger boundary-layer-removal thickness (h/δ of 1.055 as compared with 0.793) was required to obtain the maximum pressure recovery. The added boundary-layer-removal requirement and the loss of inlet mass flow might indicate a larger drag for the "cut-off" splitter-plate configuration even though a portion of the friction drag could be eliminated by removal of the splitter plate. Such a drag analysis, however, was beyond the scope of this study. The cut-off splitter plate offers a saving in airplane weight with little or no penalty on inlet pressure recovery, at least for zero angle of attack. (The data of ref. 5 indicate that a cut-off plate remains superior to the swept or "cut-back" plate throughout the angle-of-attack range.) This configuration, if operated at l/d of zero, is somewhat similar to the cowl-lip scoop configuration of reference 1. Shadowgraph and flow trace studies of the shock structure are presented in figure 14. Although some disturbance to the boundary layer ahead of the inlet lip was observed, the effect on the inlet pressure recovery was negligible.

Model B, Short Throat

After the trends obtained with model A were observed, considerably fewer configurations were investigated with the short-throat model.

Inlet pressure recovery and mass flow are shown in figures 15 and 16 for straight and swept splitter plates, respectively. It should be noted that these data are arranged less systematically than for model A; thus care should be used in interpreting trends from these figures. Peak total-pressure recoveries are summarized in figure 17. Very little subcritical stability was obtained. Generally, slightly higher performance was again obtained with the swept splitter plate. Reducing the wedge angle and moving the wedges rearward was again effective.

A comparison of the peak pressure recovery from model A, which incorporates the longer constant-area throat section, with model B may be obtained by comparing figures 7 and 10 with figure 17. Generally, when little or no boundary layer entered the inlet, such as for large values of h/δ, the maximum pressure recovery obtained with model A was slightly superior to that of model B for similar splitter-plate geometries, However, whenever considerable boundary layer entered the inlet, such as for small values of h/δ, the reverse was true. It is of interest to note that, for those configurations having straight splitter plates with the wedges in the forward position, model B attained pressure recoveries equivalent or greater than was attained with longer throat model. This occured presumably because of the previously noted tendency for boundary layer to flow up and over the straight plate and thus enter the inlet. The long-throat inlet exhibited slightly greater subcritical stability, although a margin of only 10-percent mass flow was the largest amount measured.

Wedge Pressure Drag

A drag analysis of the complete model was beyond the scope of the present investigation. However, the wedges for this investigation were instrumented with static-pressure orifices, and a pressure drag coefficient based on wedge projected area was obtained by an integration of the static pressure along the wedge face. Results of references 2 and 3 indicate that for small-angle wedges the friction drag on the boundary-layer-removal surfaces consititutes the major portion of the removal drag. For larger-angled wedges, however, friction drag becomes small compared with pressure drag. Therefore, a knowledge of the pressure drag on wedge diverters for estimating configuration drag increases is most helpful for the larger-angled wedges.

The resulting pressure drags for supercritical inlet operation are presented in figures 18 and 19 for l/d of zero and 0.48, respectively. Also presented for comparison are pressure drags which have been interpolated from the results of reference 2. Since the latter was simplified to the extent that interference effects due to the inlet external shock structure and mass-flow spillage were eliminated, these data are most applicable to supercritical inlet operation at the larger

values of boundary-layer-removal parameter. In addition, the splitter plates of reference 2 were beveled on the upper surface; whereas the splitter plates for the present investigation were beveled on the lower side, which would be expected to cause slightly higher wedge drags. The drags of the present investigation are somewhat higher than those of reference 2, although the trends are similar. At l/d of zero, agreement was best for large values of h/δ and wedge angle.

CONCLUDING REMARKS

The reduction of inlet pressure recovery with increase in wedge included angle and forward wedge movement for the half-conical inlet reported herein is more severe than was observed for a two-dimensional ramp-type inlet at lower Mach numbers (ref. 3). It is believed that Mach number, inlet geometry, Reynolds number, and so forth, are factors which affect the influence of boundary-layer shock disturbances on side-inlet performance; and it is likely that the inlet becomes more sensitive to these disturbances as the Mach number is increased and when the inlet is designed for higher degrees of external compression. It is also possible that inlets derived from axially symmetric geometries are more sensitive than ramp-type inlets because of accumulation of boundary layer in the corners.

SUMMARY OF RESULTS

An experimental investigation to study the parameters affecting wedge-type boundary-layer removal ahead of a half-conical double-shock external-compression side inlet at Mach number 2.96 yielded the following results:

1. Inlet pressure recovery and critical mass flow were improved considerably by reducing the included angle of the wedge diverter or by moving the wedge rearward from the spike tip or both.

2. When the wedge diverters were located in the forward position, swept-splitter-plate configurations generally yielded higher pressure recoveries than were obtained with splitter plates whose leading edges were normal to the free-stream direction.

3. When the wedges were located in the rearward position, neither splitter-plate configuration nor wedge included angle had much effect on the maximum inlet pressure recovery. One configuration that had no splitter plate forward of the inlet lip station

[redacted]

yielded pressure recoveries comparable with both the swept- and straight-splitter-plate configurations.

Lewis Flight Propulsion Laboratory
National Advisory Committee for Aeronautics
Cleveland, Ohio, May 26, 1954

REFERENCES

1. Piercy, Thomas G., and Johnson, Harry W.: A Comparison of Several Systems of Boundary-Layer Removal Ahead of a Typical Conical External-Compression Side Inlet at Mach Numbers of 1.88 and 2.93. NACA RM E53F16, 1953.

2. Piercy, Thomas G., and Johnson, Harry W.: Experimental Investigation at Mach Numbers 1.88, 3.16, and 3.83 of Pressure Drag of Wedge Diverters Simulating Boundary-Layer-Removal Systems for Side Inlets. NACA RM E53L14b, 1954.

3. Campbell, Robert C., and Kremzier, Emil J.: Performance of Wedge-Type Boundary Layer Diverters for Side Inlets at Supersonic Speeds. NACA RM E54C23, 1954.

4. Davis, Wallace F., Edwards, Sherman S., and Brajnikoff, George B.: Experimental Investigations at Supersonic Speeds of Twin-Scoop Duct Inlets of Equal Area. IV - Some Effects of Internal Duct Shape Upon an Inlet Enclosing 37.2 Percent of the Forebody Circumference. NACA RM A9A31, 1949.

5. Schaefer, Raymond F.: Some Design Considerations for Half-Round Side Inlets. Wright Aero. Rep. No. 1692, Supersonic Inlet Symposium, Curtiss-Wright Corp., Wood-Ridge (N. J.), Jan. 23, 1953.

TABLE I. - MODEL DIMENSIONS

Model station	Radius, R, in.			
	Centerbody		Internal lip	External lip
	Model A	Model B		
-3.80	0	0	-----	-----
-1.64	.776	.776	-----	-----
-1.116	1.134	1.134	1.500	1.500
-1.000	1.210	1.210	1.558	1.571
-.961	1.241	1.241	-----	1.595
-.900	1.280	1.280	1.600	1.631
-.800	1.336	1.336	1.636	1.695
-.700	1.378	1.378	1.658	1.742
-.600	1.406	1.406	1.678	1.769
-.500	1.423	1.423	1.689	1.796
-.400	1.432	1.432	1.697	1.822
-.300	1.434	1.434	1.701	1.849
0	1.437	1.437	1.704	1.928
1.000	1.437	1.421	↓	2.000
2.000	1.437	1.395	↓	2.000
3.000	1.428	1.349	1.704	-----
4.000	1.410	1.250	↓	-----
5.000	1.384	1.016	↓	-----
6.000	1.350	.647	-----	-----
7.000	1.287	.222	-----	-----
7.500	1.234	0	-----	-----
8.000	1.156	-----	-----	-----
9.000	.908	-----	-----	-----
10.000	.618	-----	-----	-----
11.000	.306	-----	-----	-----
12.000	0	-----	-----	-----

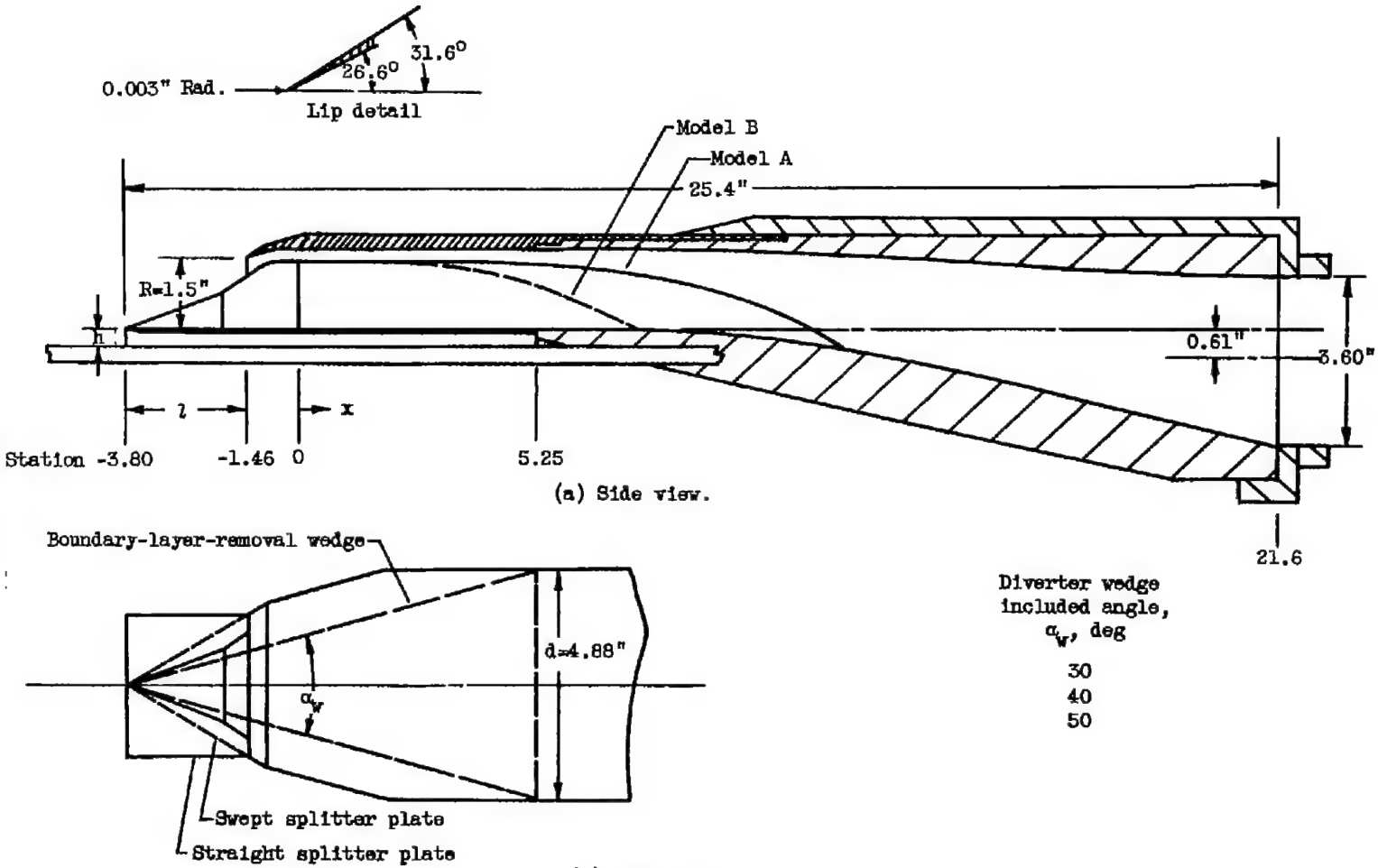

(a) Side view.

(b) Plan view.

Diverter wedge included angle, α_w, deg
30
40
50

Figure 1. - Schematic diagram of model.

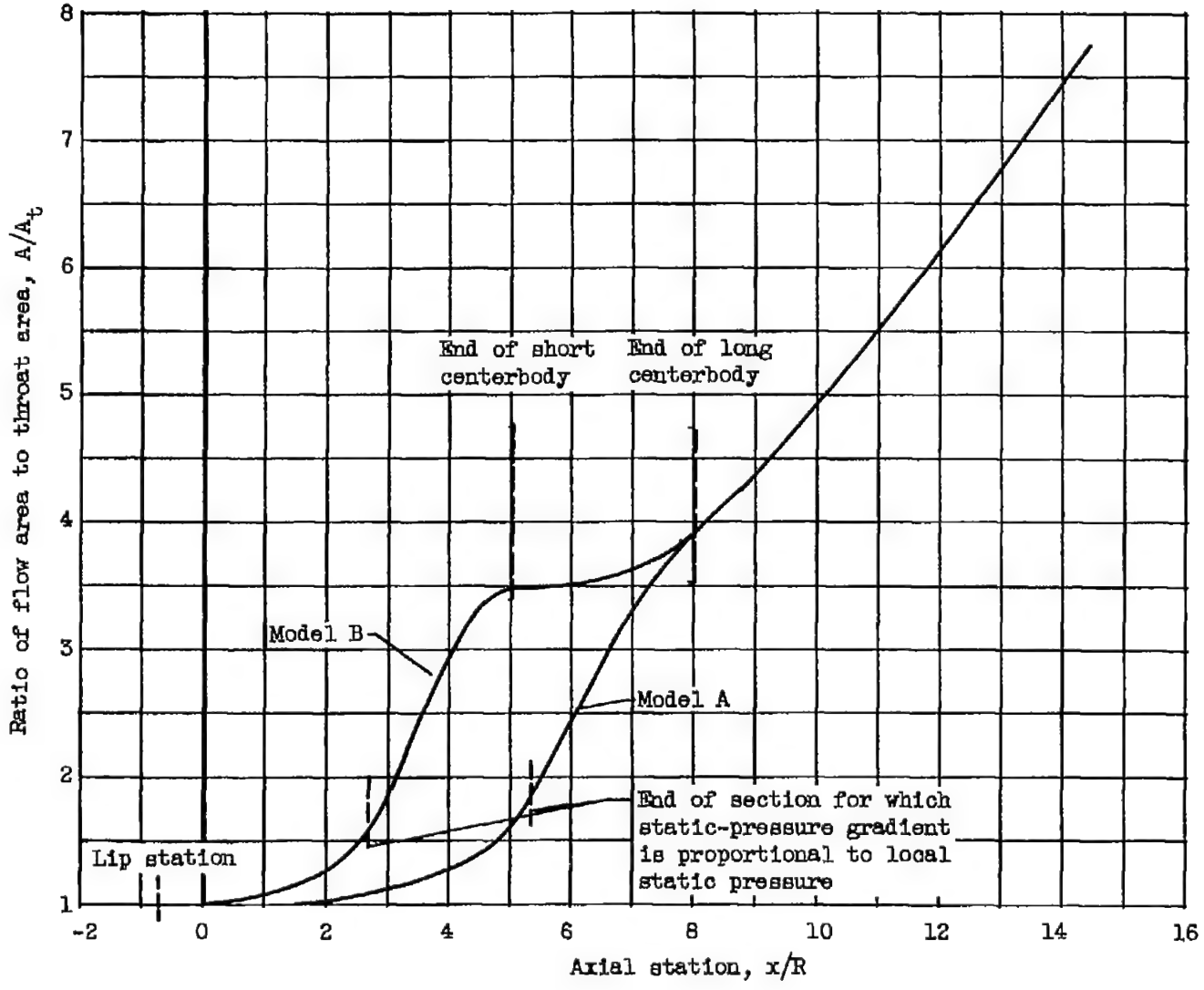

Figure 2. - Diffuser-area distributions.

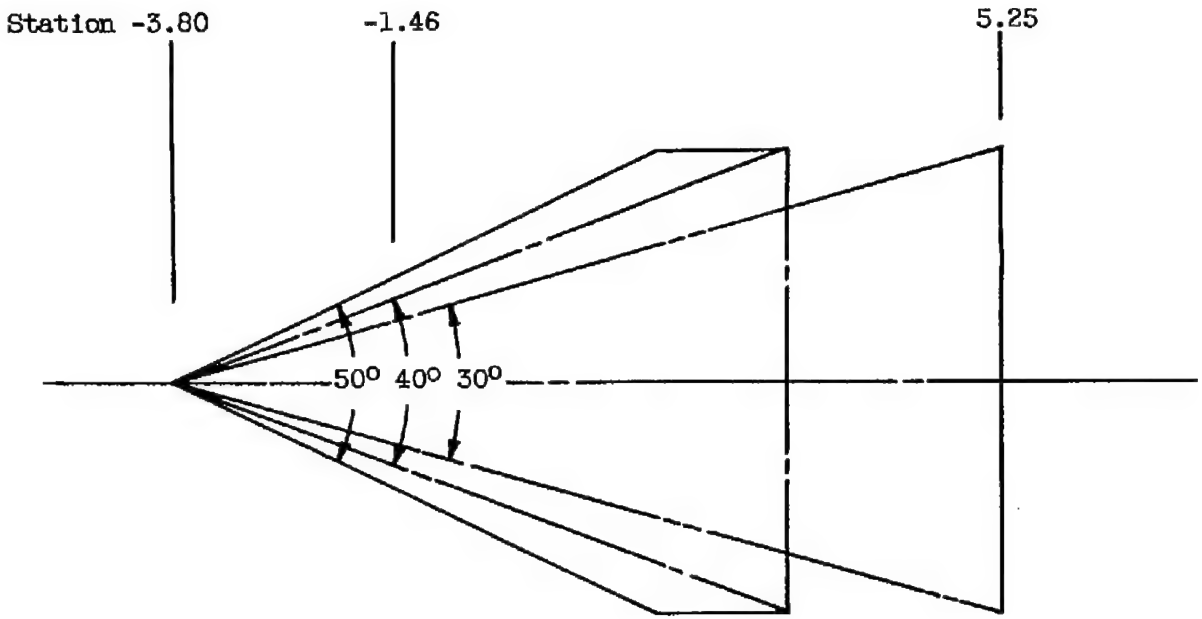

Figure 3. - Plan form of boundary-layer-removal wedges.

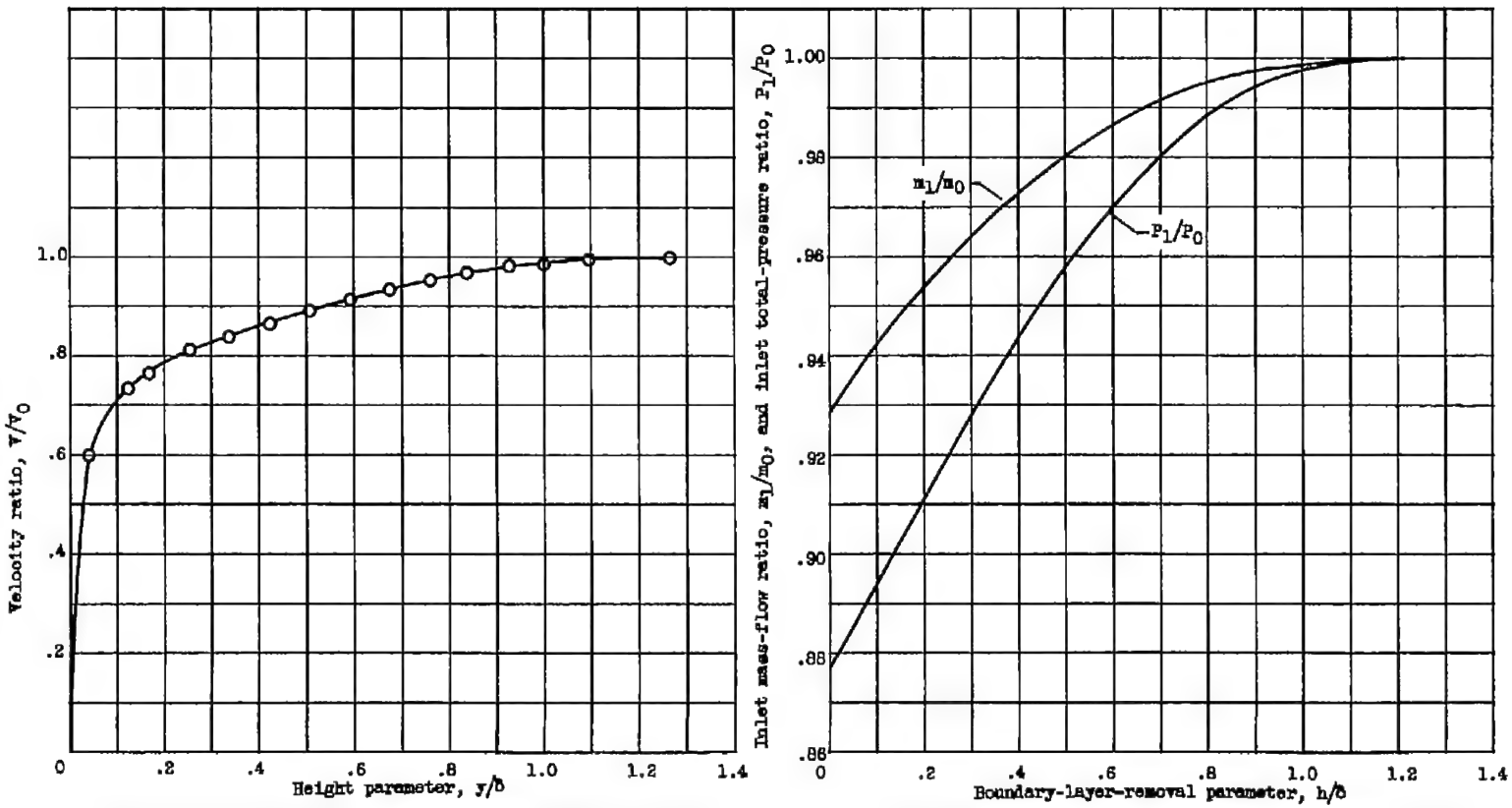

(a) Boundary-layer profile. Boundary-layer thickness, 0.257; boundary-layer form factor, 5.34; Reynolds number per foot, 1.76×10^6.

(b) Average mass flow and total pressure upstream of inlet.

Figure 4. - Boundary-layer characteristics at inlet station.

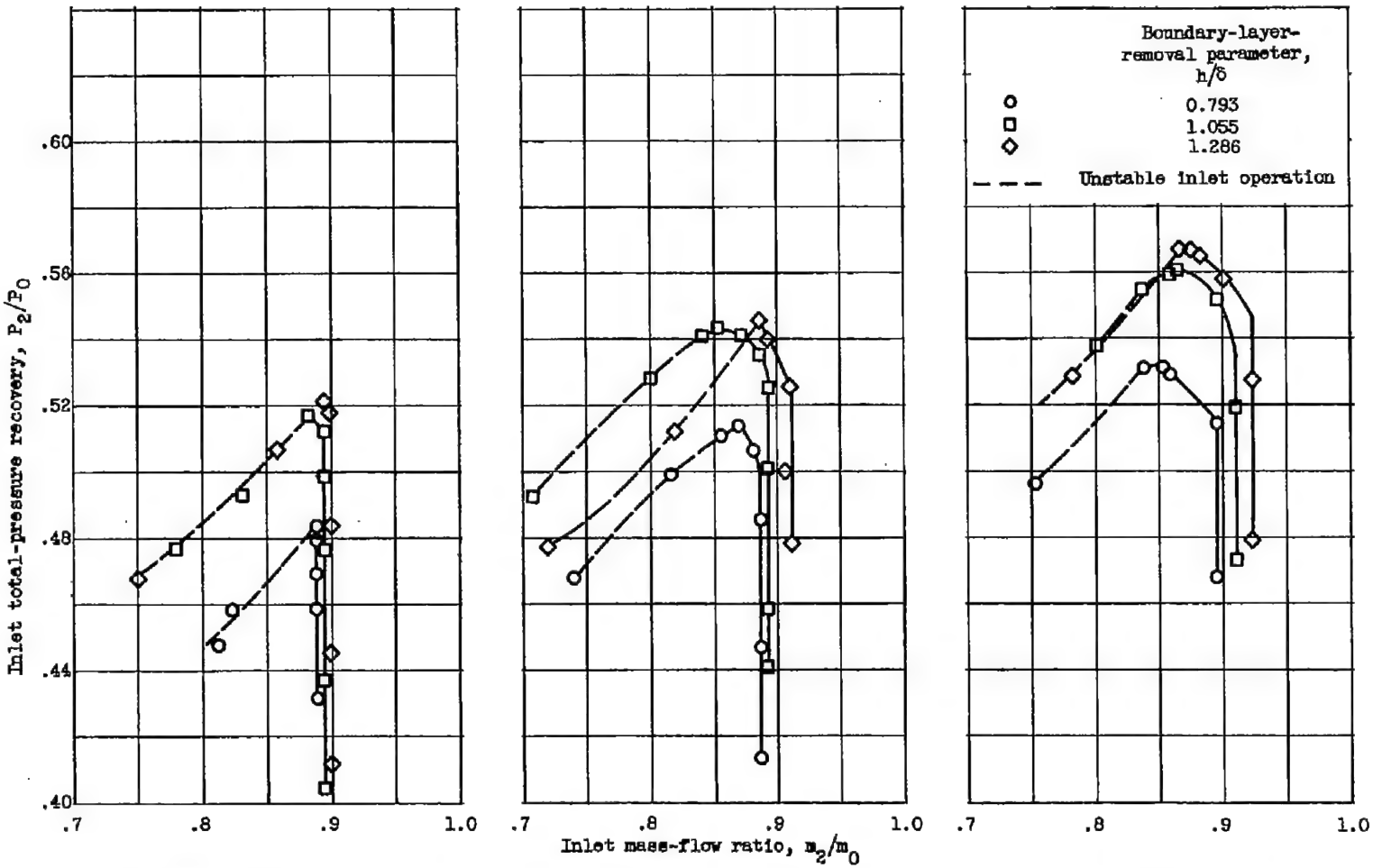

(a) Wedge included angle, 50°. (b) Wedge included angle, 40°. (c) Wedge included angle, 30°.

Figure 5. - Inlet performance with straight splitter plate. Wedges in forward position (l/d = 0); model A.

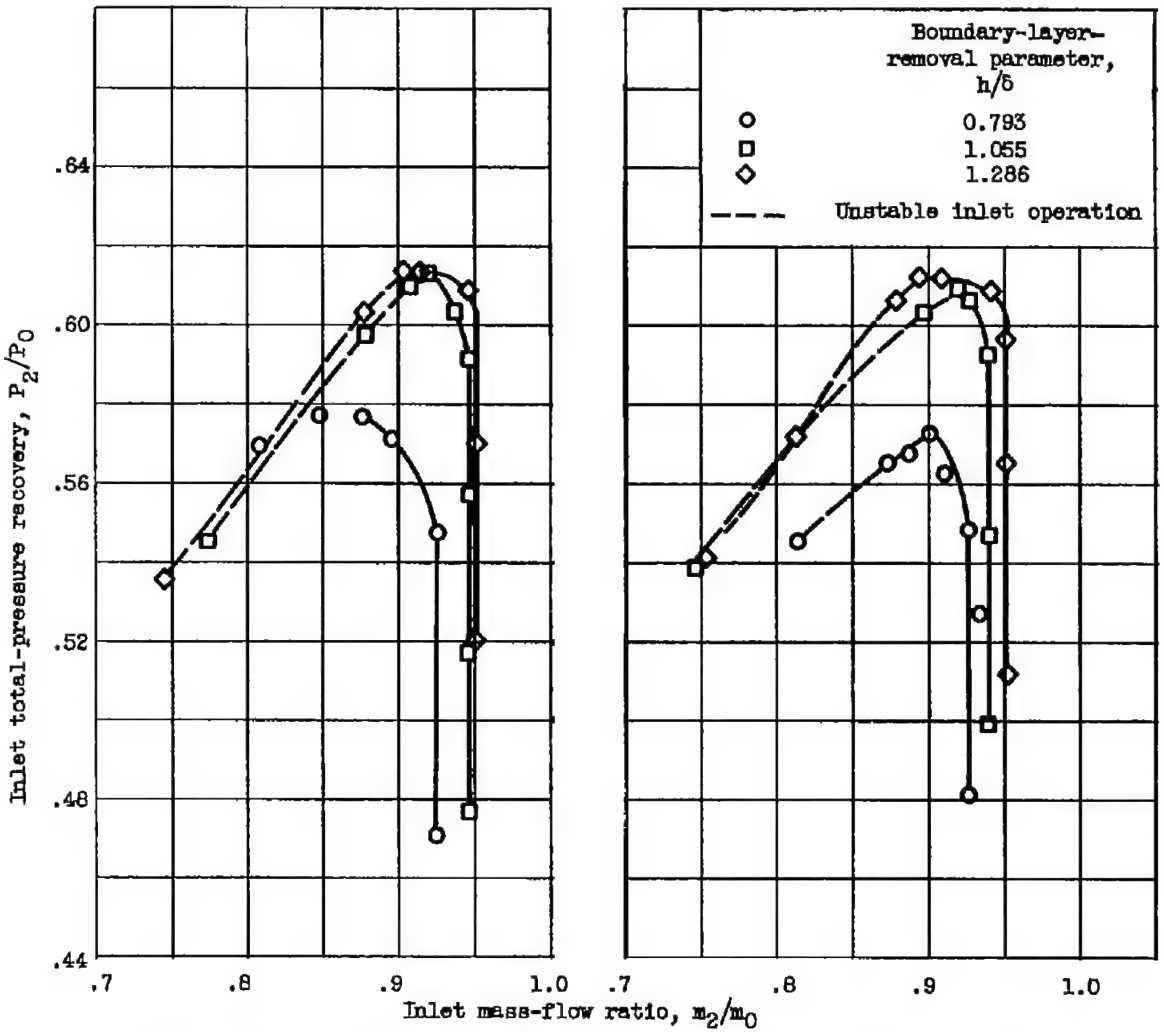

(a) Wedge included angle, 50°. (b) Wedge included angle, 40°.

Figure 6. - Inlet performance with straight splitter plate. Wedges in rearward position (l/d = 0.48); model A.

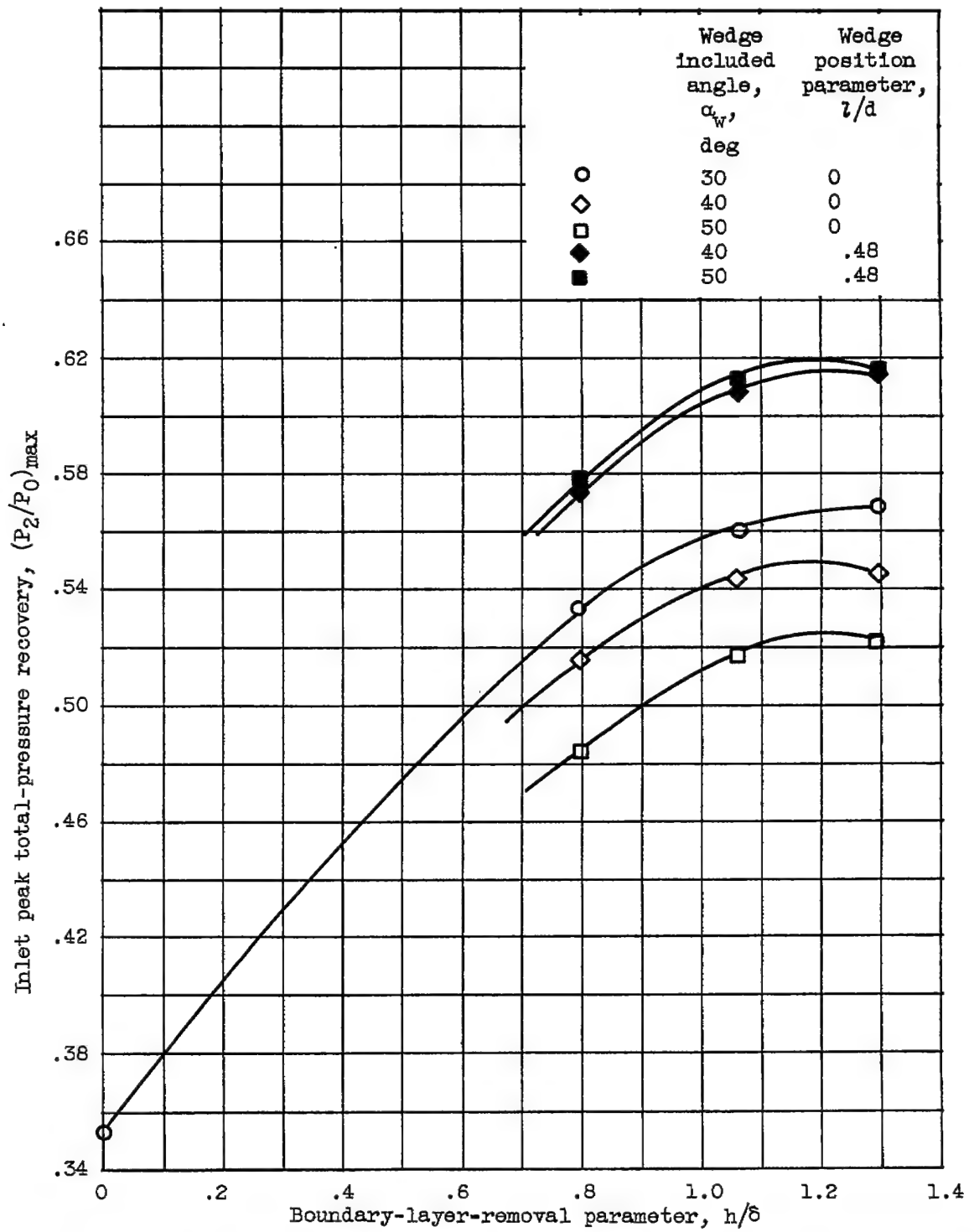

Figure 7. - Peak total-pressure recovery for straight-splitter-plate configurations. Model A.

[redacted]

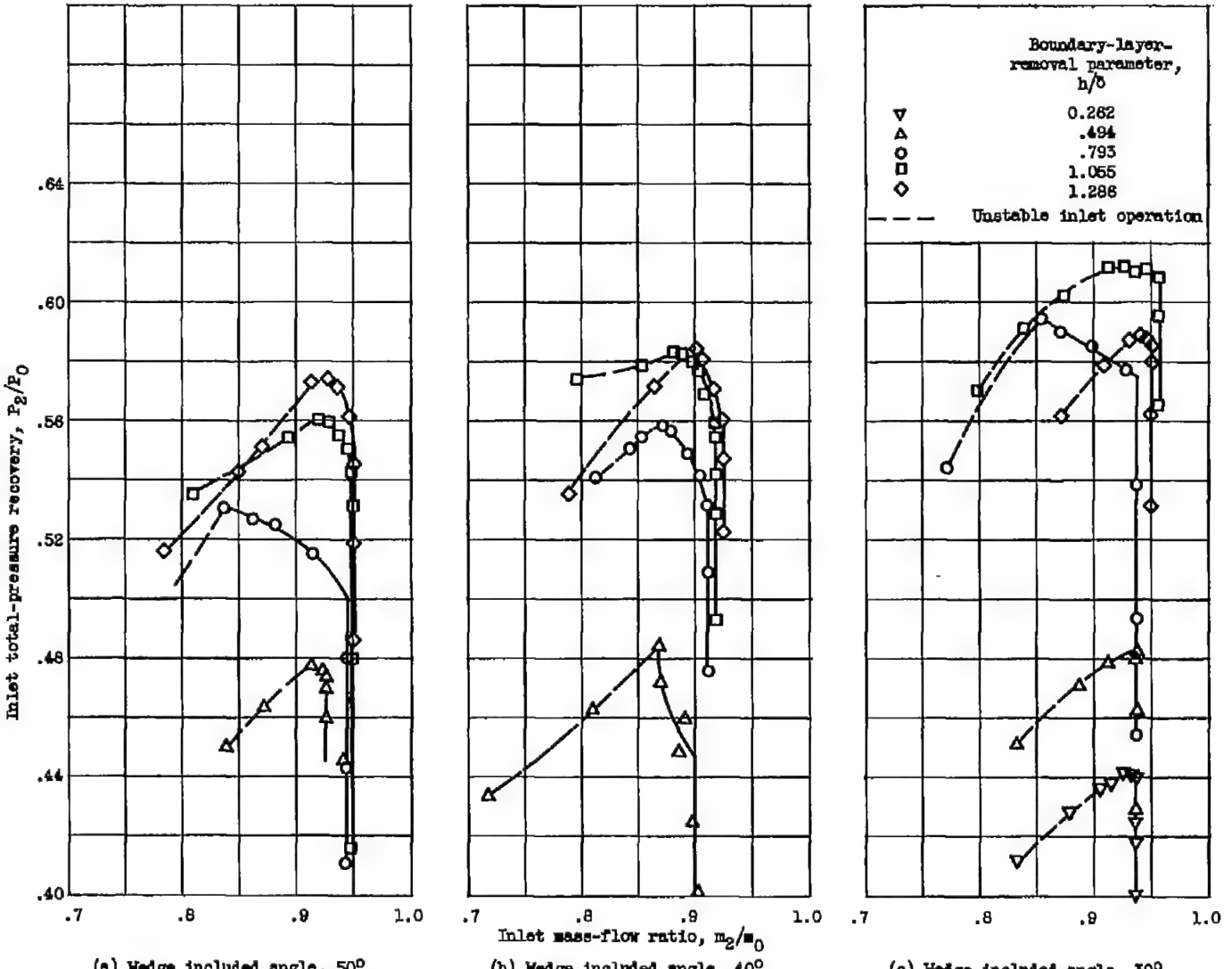

(a) Wedge included angle, 50°. (b) Wedge included angle, 40°. (c) Wedge included angle, 30°.

Figure 8. - Inlet performance with swept splitter plate. Wedges in forward position (l/d = 0); model A.

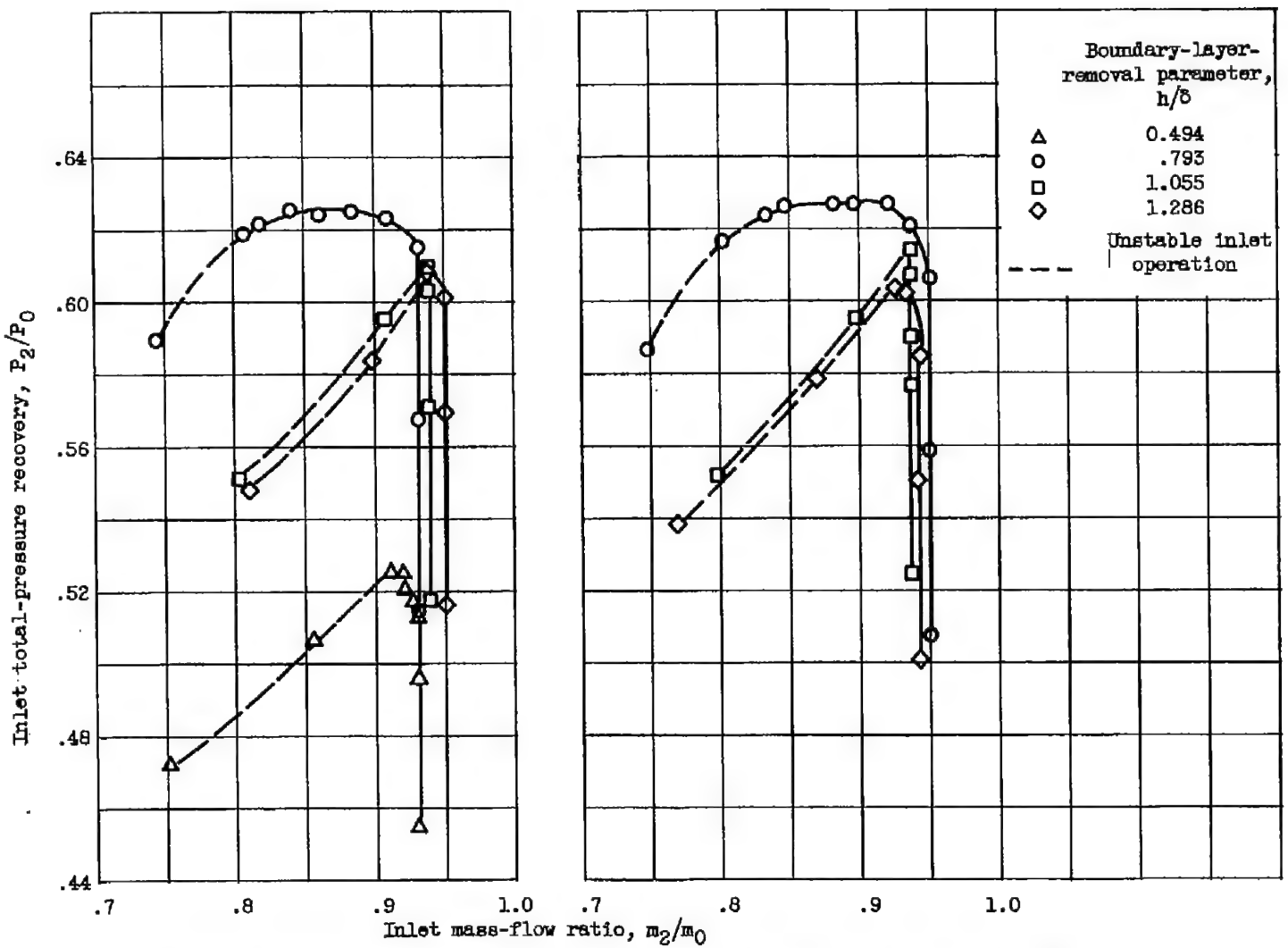

(a) Wedge included angle, 50°. (b) Wedge included angle, 40°.

Figure 9. - Inlet performance with swept splitter plate. Wedges in rearward position (l/d = 0.48); model A.

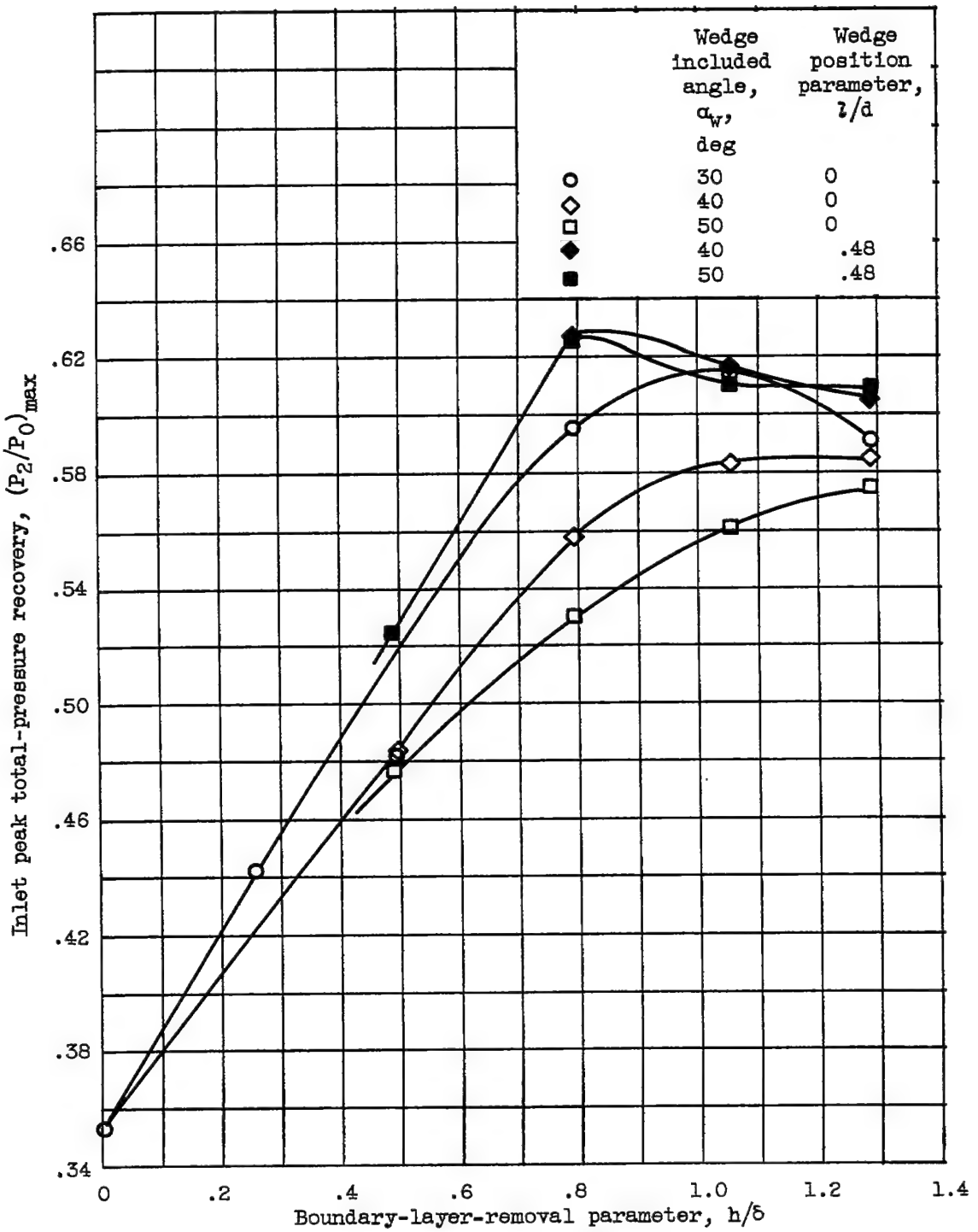

Figure 10. - Peak total-pressure recovery for swept-splitter-plate configurations. Model A.

(a) Shadowgraph

(b) Shock pattern on boundary-layer plate

Figure 11. - Inlet shock patterns for straight-leading-edge splitter plate. Wedge included angle, 40°; boundary-layer-removal parameter, 1.286; wedge position parameter, 0.

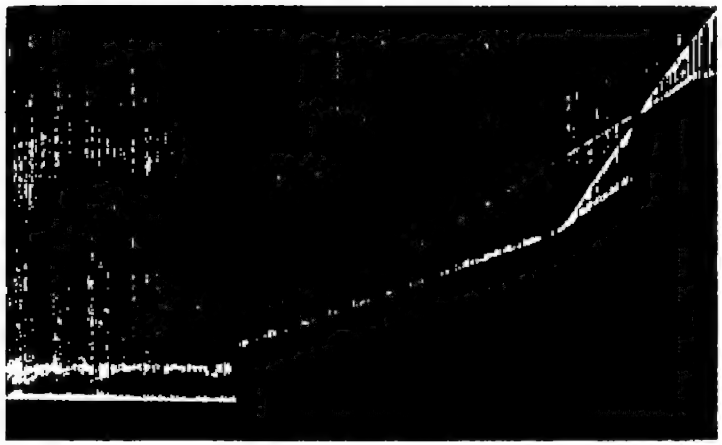

Shadowgraph

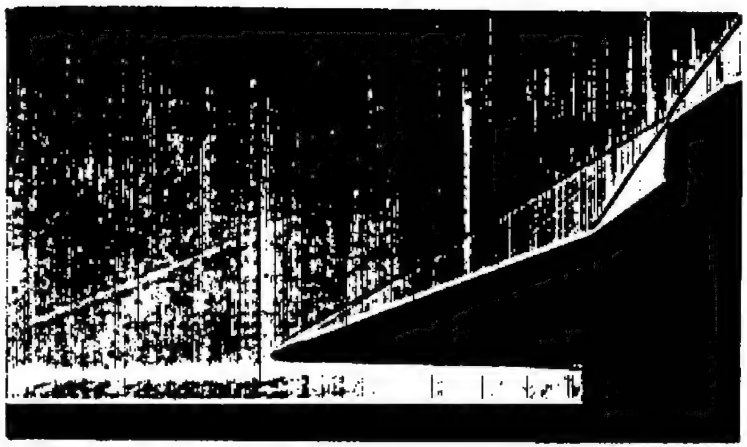

Shadowgraph

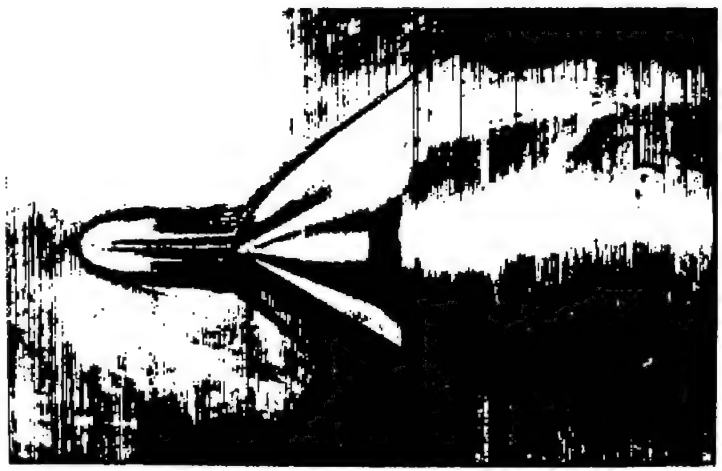

Shock pattern trace on boundary-layer plate

(a) l/d, 0.

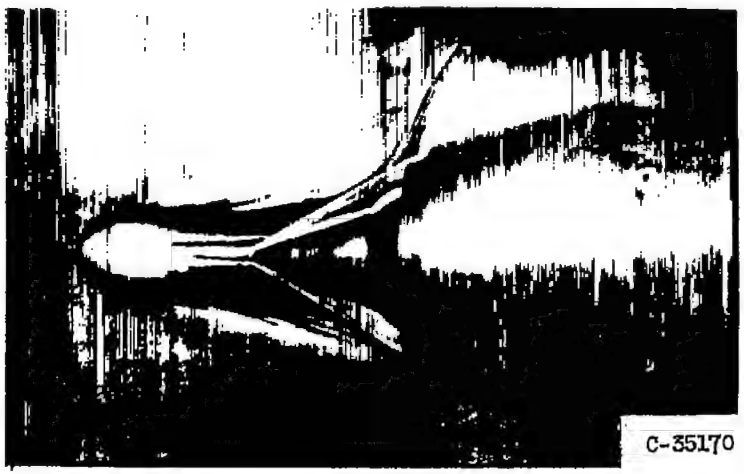

Shock pattern trace on boundary-layer plate

(b) l/d, 0.48.

Figure 12. - Comparision of shock patterns for two wedge positions l/d. Swept splitter plate; wedge included angle, 40°; boundary-layer-removal parameter, 1.286.

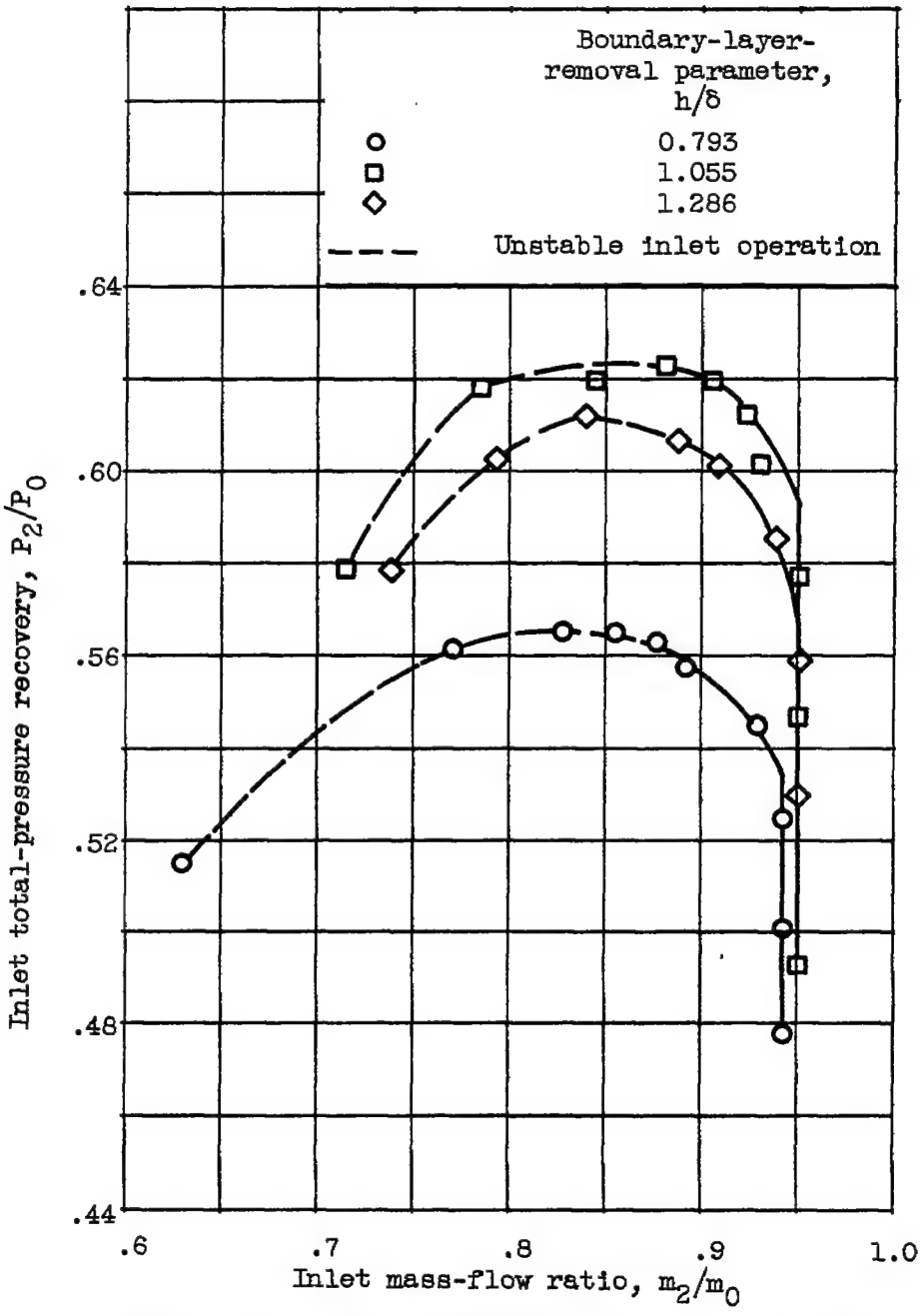

Figure 13. - Inlet performance with no splitter plate. Wedge included angle, 40°; wedge position parameter, 0.48; model A.

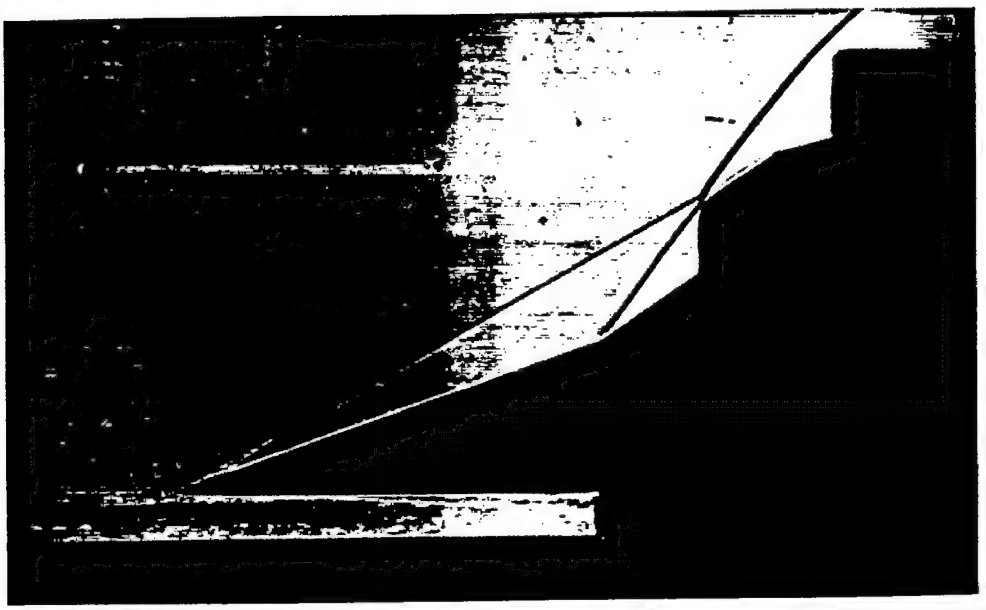

(a) Shadowgraph; inlet supercritical.

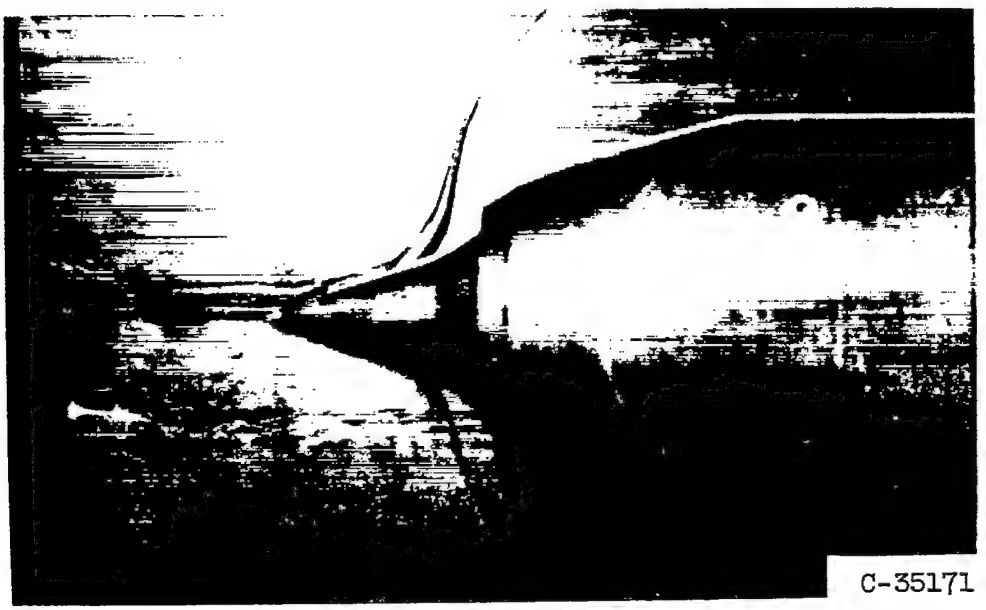

(b) Shock pattern trace on boundary-layer plate. Inlet supercritical.

Figure 14. - Inlet shock patterns for configuration with no splitter plate. Wedge included angle, 40°, boundary-layer-removal parameter, 1.055; wedge position parameter, 0.48.

[redacted]

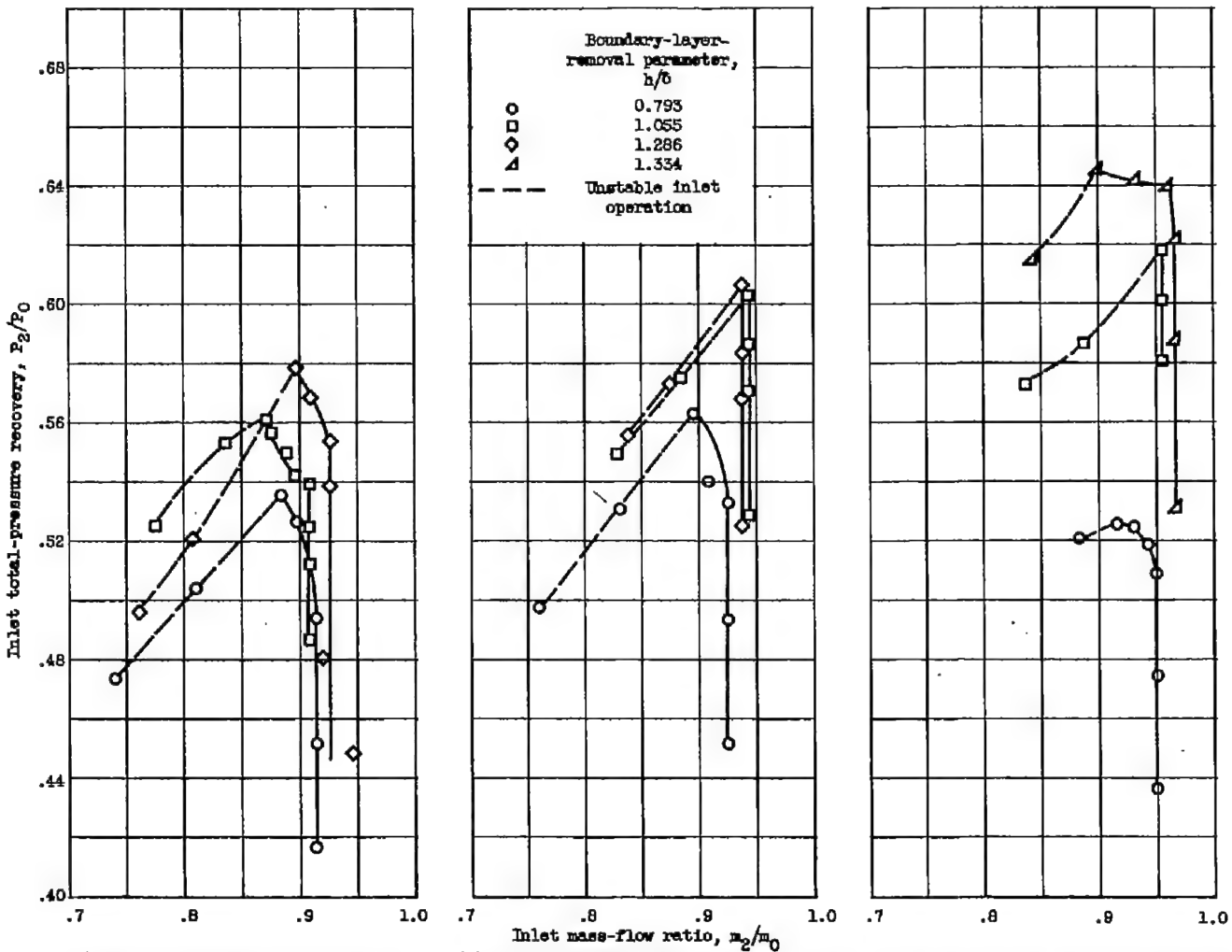

(a) Wedge included angle, 30°; wedge position parameter, 0; splitter plate at cone tip.

(b) Wedge included angle, 40°; wedge position parameter, 0.48; splitter plate at cone tip.

(c) Wedge included angle, 40°; wedge position parameter, 0.48; splitter plate at inlet lip.

Figure 15. - Inlet performance for short-throat model. Straight splitter plate.

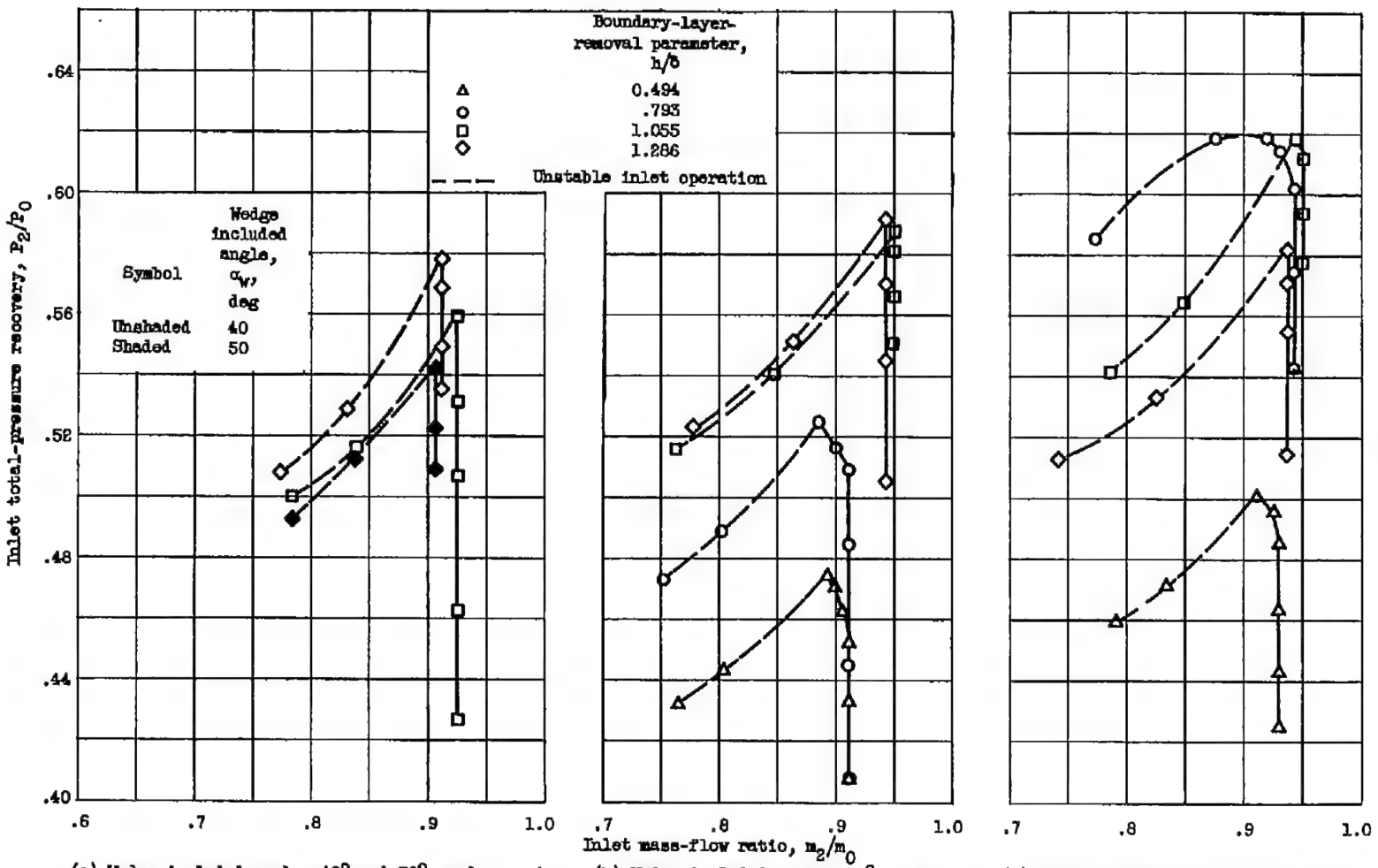

(a) Wedge included angle, 40° and 50°; wedge position parameter, 0.

(b) Wedge included angle, 30°; wedge position parameter, 0.

(c) Wedge included angle, 40°; wedge position parameter, 0.48.

Figure 16. - Inlet performance with short-throat model. Swept splitter plate.

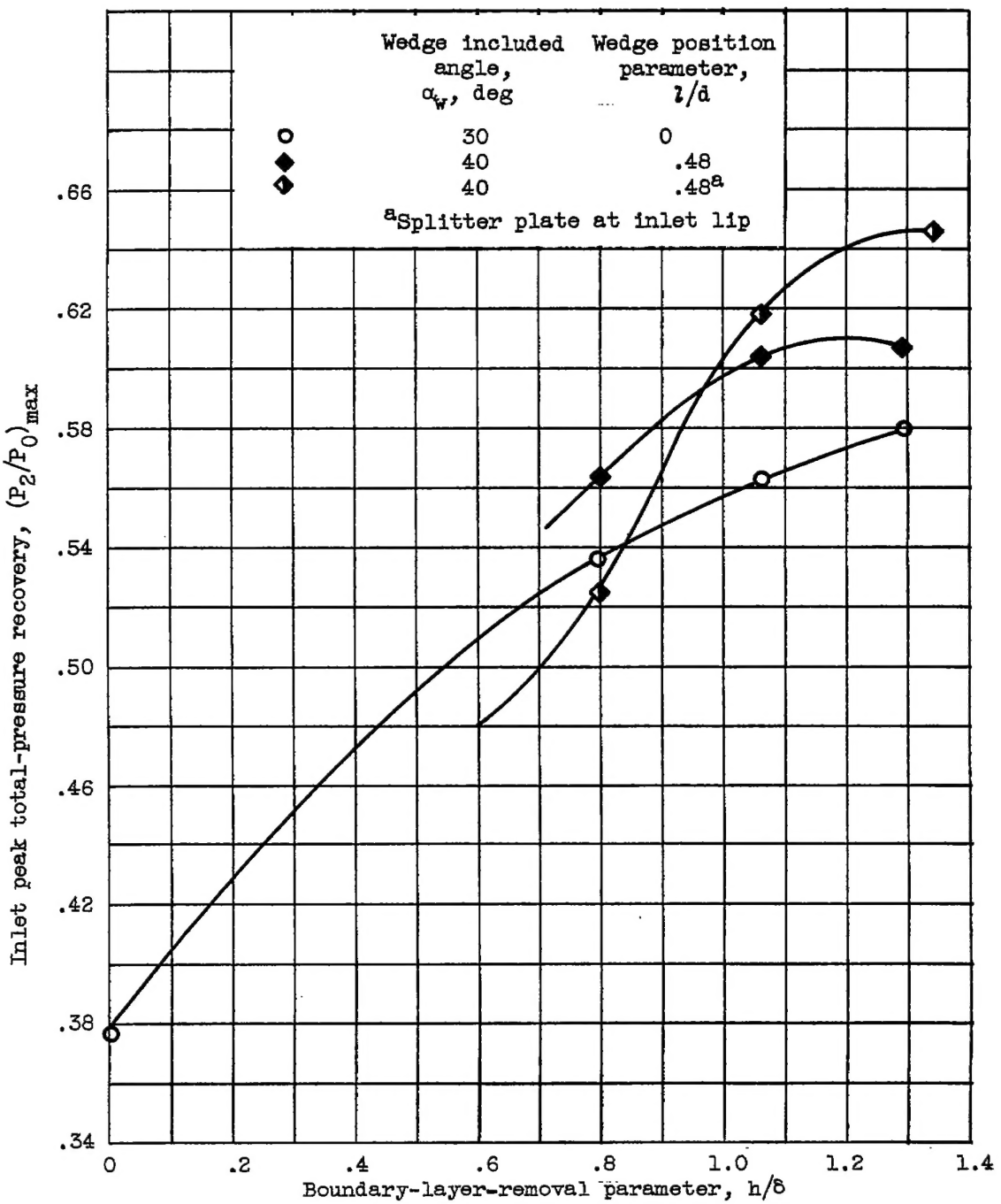

(a) Straight splitter plate.

Figure 17. - Peak total-pressure recovery for short-throat model. Model B.

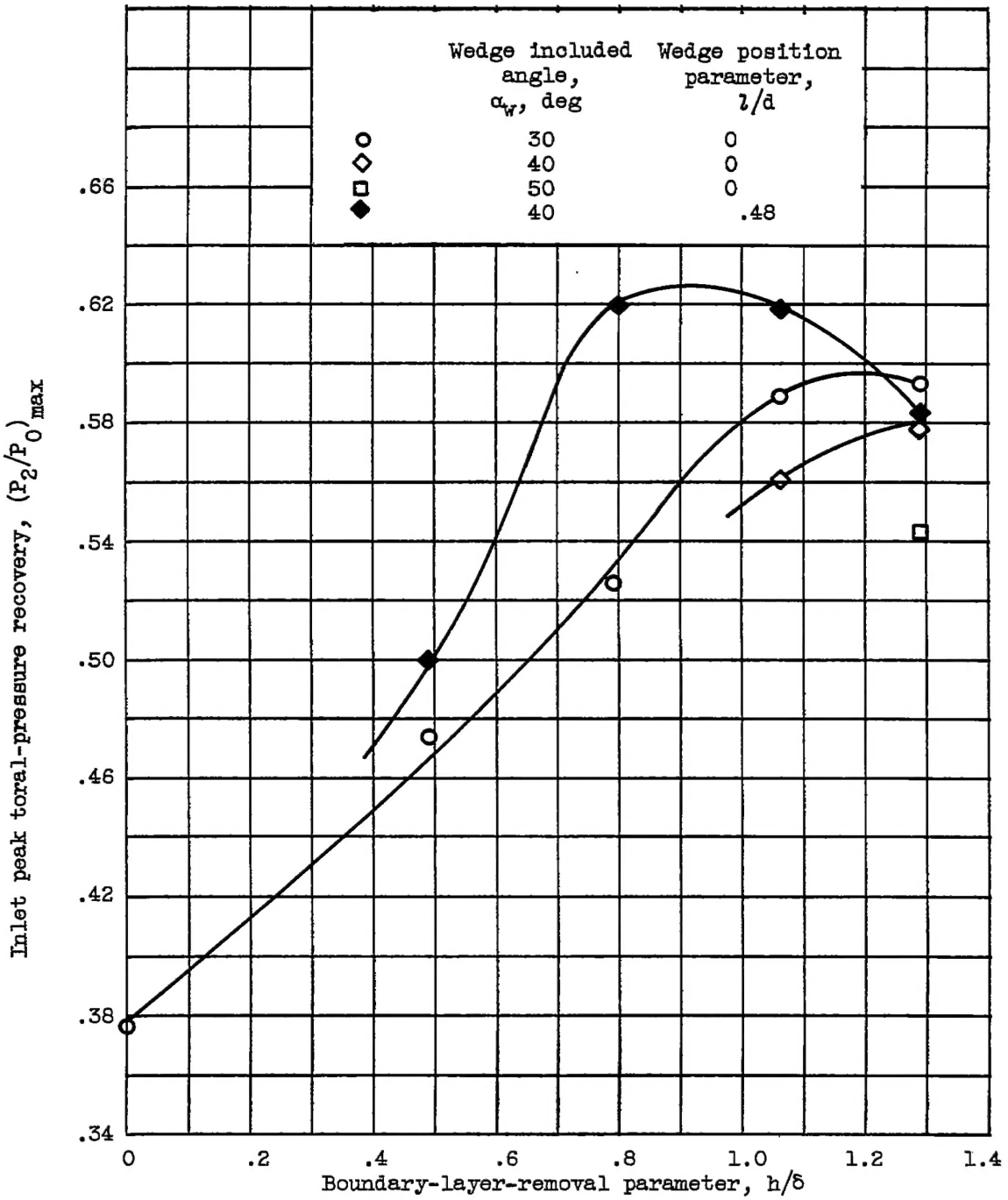

(b) Swept splitter plate.

Figure 17. - Concluded. Peak total-pressure recovery for short-throat model. Model B.

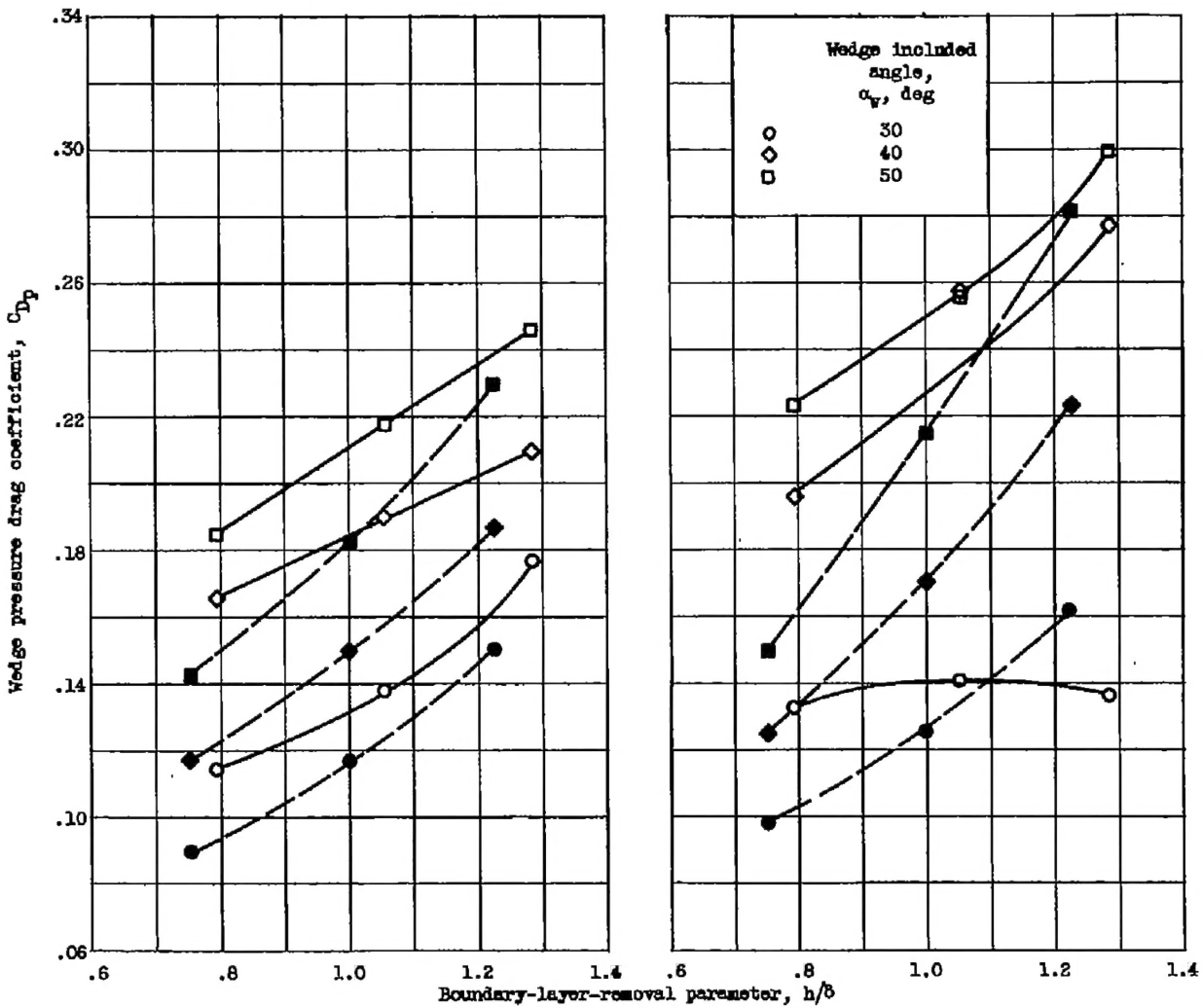

(a) Swept splitter plate. (b) Straight splitter plate.

Figure 18. - Wedge pressure drag for forward wedge position (l/d = 0). (Shaded symbols represent interpolated data from ref. 2.)

3247

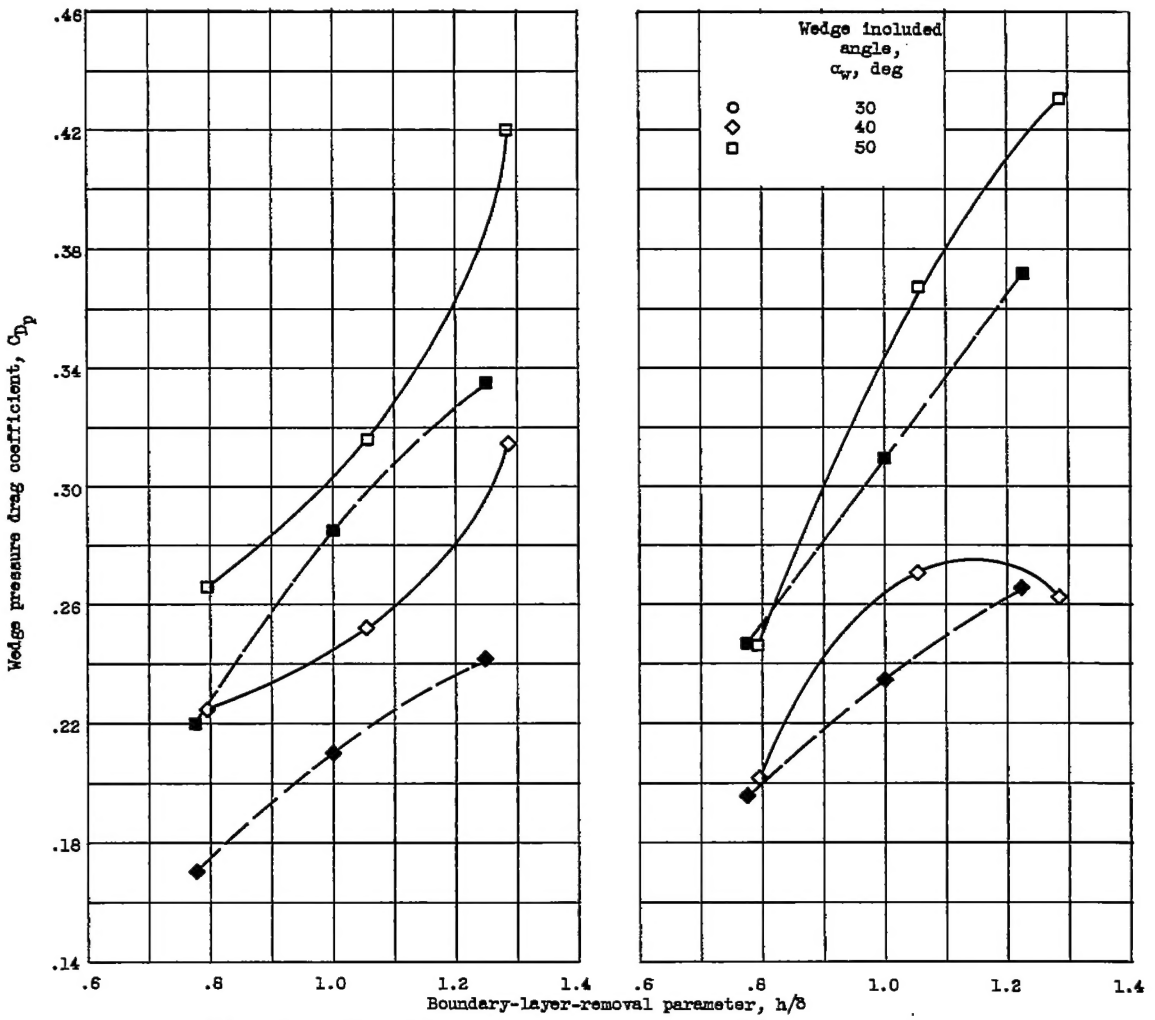

(a) Swept splitter plate. (b) Straight splitter plate.

Figure 19. - Wedge pressure drag for rearward wedge positions (l/d = 0.48). (Shaded symbols represent interpolated data from ref. 2.)

NACA-Langley - 8-2-54 - 350